Magnetic coupling and low-energy excitations in $NdGa_2$ studied by ESR

J. Dolinšek, D. Arčon, and P. Cevc
J. Stefan Institute, University of Ljubljana, Jamova 39, SLO-1000 Ljubljana, Slovenia

Z. Jagličić and Z. Trontelj
Institute of Mathematics, Physics and Mechanics, Jadranska 19, SLO-1000 Ljubljana, Slovenia

J. L. Gavilano and H. R. Ott
Laboratorium für Festkörperphysik, Eidgenössische Technische Hochschule–Hönggerberg, CH-8093 Zürich, Switzerland

Y. Aoki, H. Sugawara, and H. Sato
Department of Physics, Tokyo Metropolitan University, Minami-Ohsawa, Hachioji-shi, Tokyo 192-0397, Japan
(Received 13 April 1999)

Magnetic coupling and low-energy excitations of $NdGa_2$ were studied by electron-spin resonance (ESR) and magnetic-susceptibility measurements between room temperature and 4 K. Only the conduction-electron ESR resonance was detected, whereas the *f*-electron resonances, due to the effects of the crystalline electric field and the sf indirect exchange interactions, are shifted outside the range of the *X*-band ESR experiment. In the high-temperature regime between 300 and 100 K the ESR susceptibility appears as Pauli-like whereas below 100 K it shows an enhancement due to the sf exchange and follows the temperature dependence of the Curie-Weiss-type *f*-electron magnetic susceptibility. The *f*-electron magnetism is observed indirectly via the enhancement effect on the conduction electrons, demonstrating the importance of the exchange interactions in $NdGa_2$. Magnetization measurements with a superconducting quantum interference device magnetometer have demonstrated that the nature of the reported ferromagnetic component below 5 K is not that of a true ferromagnet. Rather, the magnetization is field induced and decays to zero after switching off the external magnetic field. A nonresonant microwave absorption, reported previously for canted antiferromagnets, was observed in the antiferromagnetic phase. [S0163-1829(99)15033-1]

I. INTRODUCTION

Rare-earth-based intermetallic compounds have raised a lot of interest in the context of gaining a fundamental understanding of magnetism in metallic conductors. Rare-earth intermetallics are simpler to understand than the $3d$-metal compounds because they show a clear distinction between the well-defined $4f$ localized moments and the conduction electrons. In $3d$ systems, on the other hand, the localized versus itinerant character of the $3d$ moments cannot always be identified in a simple way.

Among the $4f$ systems, the $R\mathrm{Ga}_2$ family (R = rare earth) of metamagnetic rare-earth intermetallic compounds attracted attention because, in spite of the relatively simple geometry of the crystal lattice, a rich variety of magnetic phenomena was observed. The Ga atom contributes three conduction electrons and both, the dipole-dipole interaction as well as the direct exchange between $4f$ electrons can, to a good approximation, be considered as negligible. One expects that the Ruderman-Kittel-Kasuya-Yoshida (RKKY)-type indirect exchange interaction serves as a reasonably good approximation for the conduction-electron-mediated interaction between the localized $4f$ electron moments, leading to magnetic order at low temperatures. However, explaining the observed metamagnetic transitions and modulated magnetic structures at low temperatures needs further considerations.

Among the $R\mathrm{Ga}_2$ systems, $DyGa_2$ (Ref. 1), $PrGa_2$ (Refs. 2,3), and $NdGa_2$ (Refs. 4–7) were studied thoroughly and revealed a rich variety of complex magnetic structures appearing in the magnetic field (H) vs temperature (T) phase diagram. Magnetic structures show an incommensurate (INC) or a long-period commensurate (C) character with a number of temperature- and field-induced metamagnetic transitions. The bulk magnetization often shows multiple field-induced steplike changes at low temperatures, which is considered as a sign of a large magnetic frustration resulting from the competition between the long-range oscillating RKKY interactions and the applied magnetic field in the presence of strong magnetocrystalline anisotropy.

In the following we concentrate on the intermetallic compound $NdGa_2$. The crystallographic unit cell contains one Nd ion situated in a high-symmetry position with the site symmetry $6/mmm$. In zero applied field $NdGa_2$ undergoes an antiferromagnetic (AFM) transition at $T_N = 9.5$ K followed by another first-order transition to a second magnetically ordered phase at $T_t = 7.5$ K. A neutron-scattering experiment[4,8] has demonstrated that the second phase shows an incommensurate AFM structure with the propagation vector $\mathbf{Q_1} = (0.136, 0, 0.014)$ in reduced units of the hexagonal reciprocal lattice and with the magnetic moments parallel to the [010] axis (i.e., perpendicular to $\mathbf{Q_1}$). In the elastic neutron-scattering spectrum at 1.9 K the peak usually associated with the third-harmonic component was not detected, suggesting that the magnetic structure is not fully of the antiphase type. Magnetization measurements indicated the existence of a

small ferromagnetic (FM) component at low temperatures. It is not clear whether this FM component results from incompletely compensated magnetic moments on defect sites or whether it is easily induced by even a small external magnetic field. The magnetic structure between T_t and T_N is the result of the coexistence of two INC substructures. The smaller part of the coexisting phases retains the low-T structure with the same wave vector $\mathbf{Q_1}$ whereas the major part shows an amplitude-modulated AFM structure with a wave vector $\mathbf{Q_2}=(0.151, 0.151, 0.035)$ and the moments pointing in the [110] direction (i.e., almost collinear with $\mathbf{Q_2}$). This relatively simple zero-field phase diagram becomes more complicated in the presence of an external magnetic field. The H-T phase diagram strongly depends on the orientation of the magnetic field with respect to the crystalline axes and exhibits a rich variety of phase transitions.[4]

The microscopic reason for the occurrence of these complex INC magnetic structures and metamagnetic states is still far from being understood. One of the problems here is a lack of a proper microscopic model that would have to include the effects of anisotropic crystalline electric fields (CEF's), an applied external magnetic field and the sf indirect exchange interaction. A good starting point here is the periodic-field model,[9] which is a mean-field model that includes all these terms and correctly reproduces some of the static physical properties like the specific heat and magnetization. However, like any mean-field model, it does not take into account magnetic fluctuations in the paramagnetic phase and collective excitations in the low-T ordered phase. Thus little can be predicted theoretically about the dynamic properties of the above systems. In addition, the experimental data on magnetic excitations are still scarce so that the dynamics remains one of the large open questions in the context of magnetism in these metallic conductors.

The renewed interest on the $NdGa_2$ compound has recently been raised due to the unusual results of specific-heat measurements[7] that showed an unexpectedly large enhancement of the linear-in-T term in C_p at temperatures below 1 K. The possible origin of this enhancement was attributed to the low-energy thermal excitations of the fluctuating Nd moments around nodes in the incommensurate AFM structure. The presence of the low-energy excitations below 1 K was confirmed also by a large linear-in-T term in the ^{69,71}Ga NMR spin-lattice relaxation rates.[10] The rates were found to be about two orders of magnitude larger than those in the nonmagnetic $LaGa_2$ compound. This enhancement effect was associated with electronic excitations between the two lowest CEF-split energy levels of the $4f$ electron system.

The above-mentioned status of affairs prompted us to perform a study—presented in this paper—of the low-energy excitations and magnetic coupling in $NdGa_2$ by electron-spin-resonance (ESR) spectroscopy, aiming at a more detailed understanding of the complex magnetism in these intermetallics.

II. EXPERIMENTAL

The ESR experiments were performed on a continuous-wave (CW) Bruker ESP 300 spectrometer operating in the X band (9.6 GHz). The spectrometer was equipped with an Oxford ESR 900 cryostat, providing temperatures between 4 and 300 K with a 0.1 K temperature stability. Magnetization and susceptibility measurements were made in a Quantum Design susceptometer using a superconducting quantum interference device (SQUID) sensor and equipped with a 6 T magnet. All measurements were performed on the same $NdGa_2$ monocrystalline sample as previously used for the measurements of the specific heat.[7]

III. CALCULATION OF ESR RESONANCES

In $NdGa_2$ there exist two kinds of ESR-resonant electrons, those forming the localized $4f$ moments and the itinerant, predominantly s-type, conduction electrons. One has to assert which of these yield an observable signal in the X-band ESR experiment. The conduction electrons are usually characterized by a g factor very close to that of free electrons ($g\approx 2$) and their X-band resonances should occur close to the free-electron resonance magnetic field of 3400 G. Because of the CEF splitting of the $4f$ electron Hund's rule ground state, the ESR resonances invoking the $4f$ electrons are not as easily predicted. One can, however, make an estimate on the basis of the known CEF energy-level diagram and the exchange field. In the hexagonal $NdGa_2$ structure, the tenfold degenerate $^4I_{9/2}$ ground-state multiplet of the Nd^{3+} ion, with a total angular momentum $J=9/2$, splits into the five doublets[4] $\Gamma_7, \Gamma_8^{(i)}$, and $\Gamma_9^{(i)}$ $(i=1,2)$ because of the crystalline electric field. Neutron-scattering data indicate that the ground state is the Γ_7 doublet, while the doublets $\Gamma_8^{(1)}$, $\Gamma_9^{(1)}$, $\Gamma_8^{(2)}$, and $\Gamma_9^{(2)}$ are approximately 8, 10, 23, and 52 K (in units of energy/k_B) above the ground state. The corresponding wave functions are given in Table I. In an external magnetic field these doublets naturally undergo a Zeeman splitting. Neglecting the sf exchange interaction for the moment, the ESR Hamiltonian relevant for the $4f$ electrons consists of a CEF and a Zeeman contribution

$$\mathcal{H}_f=\mathcal{H}_{\mathrm{CEF}}+\mathcal{H}_Z=B_2^0O_2^0+B_4^0O_4^0+B_6^0O_6^0+B_6^6O_6^6-g_J\mu_B\mathbf{H}\cdot\mathbf{J}. \tag{1}$$

The quantities B_n^m denote the CEF parameters, which for $NdGa_2$ were determined by neutron studies,[4,11] the quantities O_n^m are Stevens operator equivalents,[12] and the Landé g_J factor equals 8/11 for the Nd^{3+} ion. Since the CEF and the Zeeman terms do not commute, one has to diagonalize a 10×10 matrix (in the basis of states $|M_J\rangle$ of the total angular momentum) in order to find the field-induced splitting of the doublets $\Gamma_j^{(i)}$. The diagonalization was performed for the crystal orientation $y\|H$. Because of only a small anisotropy in the x,y plane, the result is valid also for $x\|H$. The results of the diagonalization are summarized in Table I. The allowed ESR transitions ($\Delta M_J=\pm 1$) are those within the Zeeman-split doublets $\Gamma_7, \Gamma_8^{(1)}$, and $\Gamma_8^{(2)}$. In the resonant field of free electrons ($H=3400$ G) the splittings are 0.83, 0.64, and 0.65 K, respectively. In the CW experiment the magnetic field is swept from 0 to 10 kG at a constant irradiation frequency $\nu=9.6$ GHz, corresponding to a microwave photon energy of 0.45 K. The $4f$ resonances are thus expected at fields of 1890, 2440, and 2410 G, respectively, and should thus be observable in an X-band experiment. Due to the low photon energy, only the intradoublet transitions

TABLE I. (a) CEF states, (b) energies and (c) wave functions (Ref. 15) of $4f$ electrons in $NdGa_2$ in the absence of magnetic field. Column (d) shows the Zeeman splitting of the CEF doublets in a magnetic field $H=3400$ G and column (e) the corresponding ESR resonant field at $\nu=9.6$ GHz for the allowed X-band transitions [column (f)] in the absence of sf exchange. The resonance frequencies in the presence of an exchange field 20 kG are listed in (g).

(a) CEF states Γ_i	(b) Energies E_i (K)	(c) Wave functions ψ_i	(d) Zeeman splitting ($H=3400$ G) ΔE_i (K)	(e) ESR resonant field at $\nu=9.6$ GHz in the absence of sf exchange H (G)	(f) ESR transitions $\Delta M_J=\pm 1$ allowed	(g) ESR resonance frequencies in the presence of exchange field 20 kG ν(GHz)
$\Gamma_9^{(2)}$	51.6	$0.12\|\pm 3/2\rangle+0.99\|\mp 9/2\rangle$	~ 0		No	
$\Gamma_8^{(2)}$	23.2	$0.78\|\pm 5/2\rangle+0.63\|\mp 7/2\rangle$	0.65	2410	Yes	77.6
$\Gamma_9^{(1)}$	10.0	$0.12\|\pm 9/2\rangle-0.99\|\mp 3/2\rangle$	6.8×10^{-3}		No	
$\Gamma_8^{(1)}$	7.8	$0.63\|\pm 5/2\rangle-0.78\|\mp 7/2\rangle$	0.64	2440	Yes	67.2
Γ_7	0	$\|\pm 1/2\rangle$	0.83	1890	Yes	96.2

can be excited, because the interdoublet energy splittings of several K are much too large in comparison with the chosen frequency.

The indirect exchange interaction between the f electrons has a profound effect on the $4f$ resonances. A simple estimate of this effect can be made by a mean-field treatment where one replaces the actual exchange field by a mean molecular field $\mathbf{H}_{\rm mol}$ that adds to the external field $\mathbf{H}$. Though $H_{\rm mol}$ is not known precisely for $NdGa_2$, one can find its order of magnitude by assuming that $H_{\rm mol}$ points in the same direction as H and determining the value of the external field that completely polarizes the spins at temperatures well below T_N. This polarizing field value sets the upper limit for the exchange field and can be easily determined from the value of the field in the M vs H curve above which the saturation of the magnetization occurs. In $NdGa_2$ this field is about 20 kG (see Fig. 8 in Ref. 4). The same order of magnitude is also obtained from the ordering temperature using equation $\mu_{\rm eff}H_{\rm mol}=k_BT_N$ that yields $H_{\rm mol}\approx 40$ kG for $\mu_{\rm eff}\approx 3.5\,\mu_B$ and $T_N=9.5$ K. In order to find the $4f$ resonances in the presence of the exchange field, the Hamiltonian of Eq. (1) was diagonalized for $H=20$ kG (Table I). The diagonalization yields the energy splittings of the Γ_7, $\Gamma_8^{(1)}$, and $\Gamma_8^{(2)}$ doublets of 3.7, 3.2, and 4.6 K, respectively. The corresponding ESR resonance frequencies are 77.6, 67.2, and 96.2 GHz, far outside of the available experimental range, so that the $4f$ resonances cannot be observed directly. It is, however, still possible to observe the f-electron excitations indirectly via the conduction-electron resonance, because the sf exchange coupling results in an enhancement of the conduction-electron susceptibility at low temperatures. Here it is also worth noting that at least at low temperatures, the modulation of the magnetic structure quite likely implies a wide distribution of molecular fields $H_{\rm mol}$, so that the direct f-electron ESR transitions might, in principle, be too broad to be detected. In any case, the missing f resonances can be considered as a demonstration of the importance of the exchange interactions in $NdGa_2$.

IV. RESULTS AND DISCUSSION

The ESR experiments were performed on an $NdGa_2$ monocrystalline sample (with its $[0\bar{1}0]$ axis oriented parallel to the external magnetic field), in the temperature interval from 300 to 4 K. A selected collection of spectra is shown in Fig. 1. Upon cooling from room temperature to 4 K the electronic g factor [Fig. 2(a)] showed a small variation with the values in the range between 2.02 and 2.15. These values are typical for itinerant conduction electrons, supporting the above hypothesis that the $4f$ resonances cannot be observed directly in the X-band ESR experiment. In Fig. 2(b) the peak-to-peak width $\Delta H_{\rm pp}$ of the derivative spectra is shown. In the interval from 210 to 130 K $\Delta H_{\rm pp}$ decreases and exhibits a minimum at 130 K. Such narrowing of the ESR line on cool-

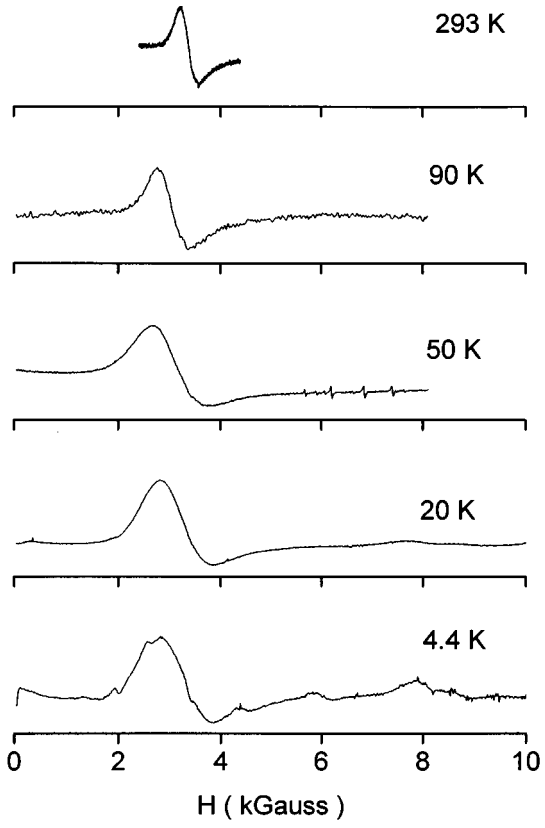

FIG. 1. X-band ESR spectra of a $NdGa_2$ monocrystalline sample between room temperature and 4 K.

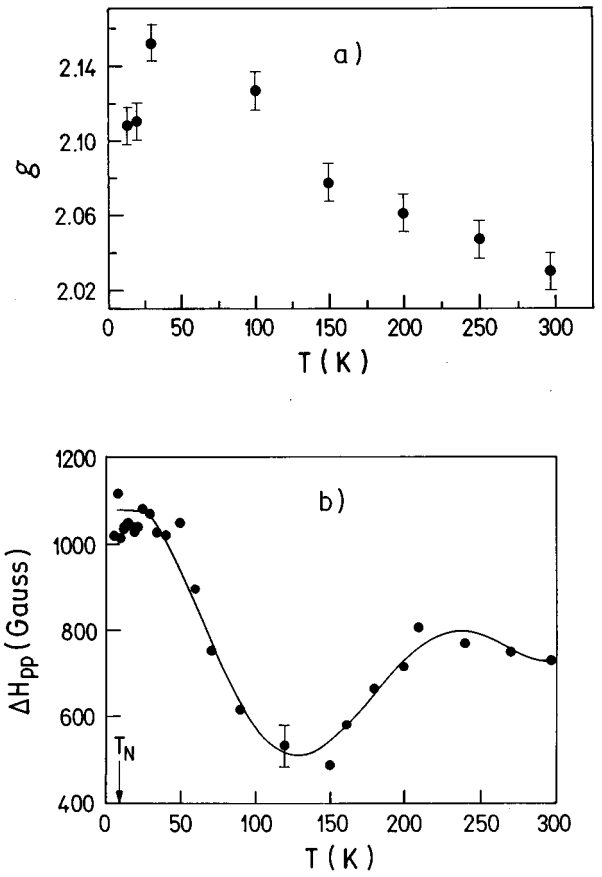

FIG. 2. (a) Temperature dependence of the g factor of the ESR spectra of $NdGa_2$. (b) peak-to-peak width ΔH_{pp} of the ESR derivative spectra as a function of temperature. The solid line is a guide for the eye.

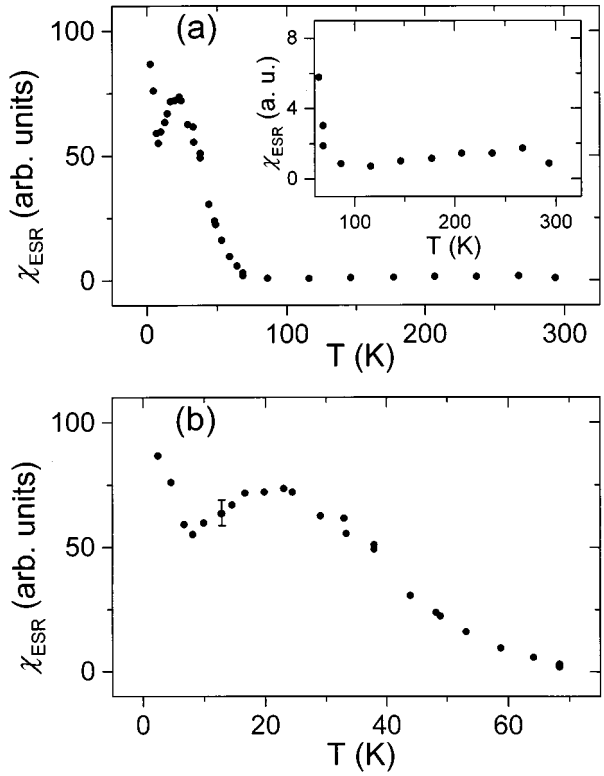

FIG. 3. (a) ESR susceptibility of an $NdGa_2$ monocrystal ($[0\bar{1}0]$ axis parallel to the magnetic field) in the temperature interval between 300 and 4 K. The inset shows χ_{ESR} between 300 and 70 K on an expanded temperature scale. (b) The low-T part of χ_{ESR}, showing details around the AFM transition.

ing in metallic samples usually occurs as a consequence of the lifetime broadening mechanism.[13] The lifetime contribution to the linewidth can be written as $\Delta H_{pp}^{\tau}=\hbar/(g\mu_B\tau)$, where τ represents the lifetime of the ESR excited state that increases at lower temperatures so that ΔH_{pp}^{τ} decreases. Below 130 K, ΔH_{pp} increases again and saturates at a value $\Delta H_{pp}=1050\,\mathrm{G}$ below 50 K. This increase originates from the sf indirect exchange interaction as will be demonstrated below by comparing the ESR and magnetic susceptibilities.

The ESR susceptibility is obtained from the intensity I_{ESR} of the absorption line and is defined by the linear relation $I_{ESR}=\chi_{ESR}H$. Here I_{ESR} represents the relative intensity of the ESR signal so that χ_{ESR} cannot be analyzed quantitatively on an absolute emu/mol scale, but its temperature dependence is of significance. The ESR susceptibility of $NdGa_2$ is displayed in Fig. 3(a). In the temperature region between room temperature and 4 K, two different regimes may be identified. In the high-temperature part between 300 and 80 K [see inset in Fig. 3(a)], χ_{ESR} is only insignificantly T dependent, at best with a small *decrease* towards low temperatures. Below 80 K χ_{ESR} starts to increase in a Curie-Weiss-like manner [Fig. 3(b)]. The behavior of χ_{ESR} in the high-T regime can, to a good approximation, be ascribed to the Pauli paramagnetism of conduction electrons with the susceptibility of the form $\chi_c=\mu_B^2 g(\varepsilon_F)$, where $g(\varepsilon_F)$ is the density of conduction electron states at the Fermi level. Such a Pauli-like ''background'' susceptibility was also observed in the nonmagnetic $LaGa_2$ compound.[5]

In contrast to χ_{ESR}, the bulk magnetic susceptibility χ [Fig. 4(a)] displays a very different behavior. As usually observed for this type of compound, $\chi(T)$ shows a Curie-Weiss-type increase from room-temperature down to about 10 K. This behavior is clearly reflected in the χ^{-1} vs T plot in the inset of Fig. 4(a), so that $\chi(T)$ can unambiguously be attributed to the paramagnetism of the $4f$ electrons. The Curie-Weiss parameters in the paramagnetic state are $\theta=15\,\mathrm{K}$ and $\mu_{eff}=3.51\mu_B$. The anomalies in $\chi(T)$ in the vicinity of the AFM transition at 9.5 K are displayed on an expanded temperature scale in Fig. 4(b). Here we mention that similar magnetic susceptibility data of $NdGa_2$ have recently been published.[4] We include our data here because χ was measured on the same crystal and at the same orientation as χ_{ESR}, thus allowing for a direct comparison.

The comparison of χ and χ_{ESR} suggests the following explanation of the temperature dependence of the ESR linewidth ΔH_{pp} and χ_{ESR} below 80 K. The f and conduction electrons are coupled through the sf exchange so that one observes an enhanced susceptibility of the conduction electrons of the form

$$\chi_{ESR}=\chi_c[1+C(T)\chi_{4f}]. \tag{2}$$

Here χ_c is the conduction-electron susceptibility in the absence of exchange with the f electrons and $C(T)$ is the sf coupling constant that may be temperature dependent. Upon

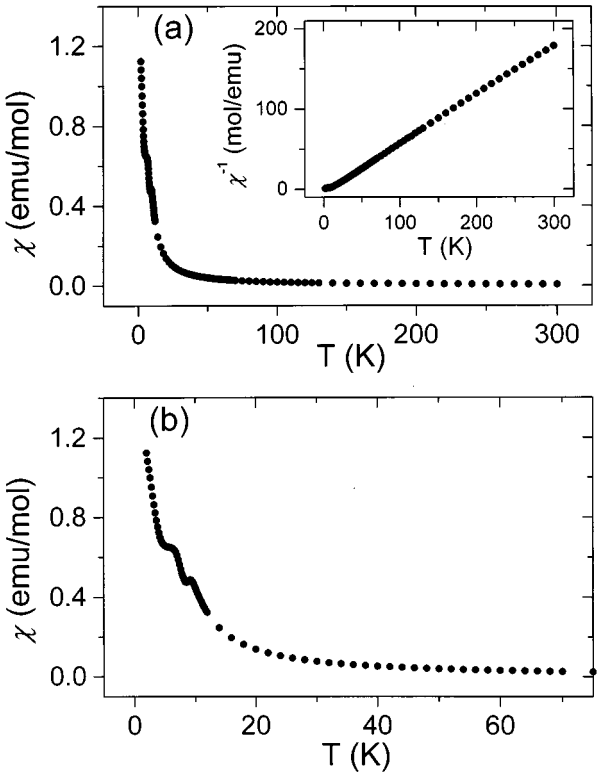

FIG. 4. (a) Bulk magnetic susceptibility χ of an $NdGa_2$ monocrystal ($[0\bar{1}0]$ axis parallel to the magnetic field) measured in a field $H=500$ G as a function of temperature. The inset shows the χ^{-1} vs T plot. (b) The low-temperature part of $\chi(T)$, exhibiting anomalies in the AFM phase.

cooling the $4f$-electron susceptibility increases in a Curie-Weiss manner and once it is large enough, it provides the dominant contribution to the intensity and width of the conduction-electron ESR line via the sf coupling. The coupling induces an enhancement of the conduction-electron susceptibility so that the T dependence of χ_{ESR} [and $C(T)$] below 80 K predominantly follows that of χ_{4f}. The f-electron magnetism is thus observed indirectly via the enhancement effect on the conduction electrons, probed by ESR. Our results therefore demonstrate the importance of exchange interactions and their influence on the magnetic phenomena observed in $NdGa_2$. Here we mention that the ESR spectrum width saturates already at 50 K, i.e., far above the AFM transition, and no further changes are observed on crossing T_N. This suggests that the external magnetic field of the ESR experiment induces partial polarization of the moments and smears out the AFM phase transition. This smearing seems also to be responsible for the fact that fine details in the magnetic susceptibility χ below 10 K are not mirrored in χ_{ESR}.

In view of the reported weak ferromagnetic component[4] that is claimed to coexist with the AFM order at temperatures below about 5 K, one is faced with the question whether the FM component represents a true ferromagnetic state with spontaneous local magnetic fields or whether these fields are induced by an external magnetic field. In a system with a large magnetic frustration like $NdGa_2$, the second possibility is likely to occur as already small external fields may induce a significant moment polarization. The above

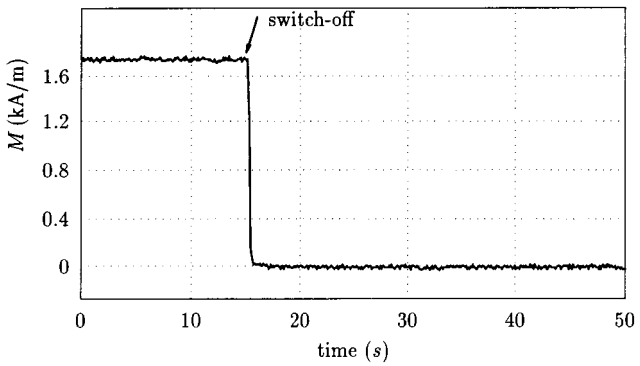

FIG. 5. Time decay of the $NdGa_2$ bulk magnetization after switching off the magnetic field, measured by a SQUID magnetometer at 4.2 K.

ESR experiments were performed in a relatively high field with the center of absorption at 3400 G and can thus not give the answer to this question. To clarify this point we performed an experiment where the sample was placed in a dc SQUID magnetometer at 4.2 K and was magnetized with a field of 100 G. After the equilibrium was reached, the field was suddenly turned off and the time decay of the magnetization was recorded. The magnetization decayed to exact zero (Fig. 5) in a time of less than 2 s, demonstrating that no remanent magnetization exists in zero field at this temperature.

Another interesting phenomenon detected in our ESR experiments below the AFM transition, is the appearance of

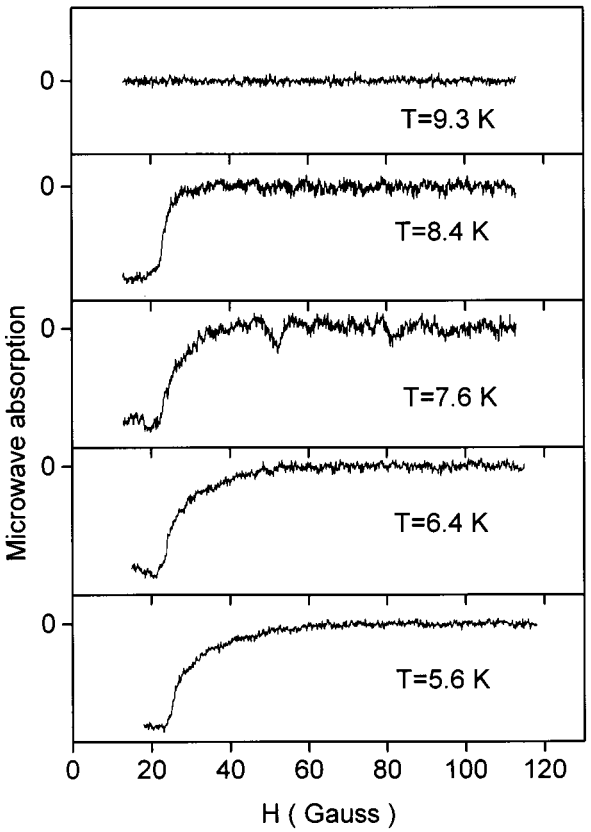

FIG. 6. ESR signals showing a nonresonant microwave (9.6 GHz) absorption at zero magnetic field in the magnetically ordered phase of $NdGa_2$.

nonresonant (9.6 GHz) microwave absorption at zero magnetic field. In this experiment the ESR magnetic-field sweep started at zero (in fact not exactly at zero but at a value of about 20 G, determined by the residual field of the magnet poles) and the microwave absorption in the sample was observed in a narrow range of the order of a few ten Gauss around the field zero, thus in the regime where the ESR resonance condition is not fulfilled. This nonresonant absorption was observed below T_N (Fig. 6) in the magnetically ordered phase of $NdGa_2$, whereas it was absent above. Such nonresonant absorption was previously reported in rare-earth-containing canted antiferromagnets.[14] There this effect was attributed to the spontaneous moments that undergo reorientations upon a temperature change and respond quasistatically to alternating magnetic fields at microwave frequencies. It is due to some kind of low-energy magnetic excitations. Similar arguments are likely valid also for explaining our observation on $NdGa_2$. The complicated magnetic structure, however, prevents us from giving a more detailed description of this phenomenon at present.

V. CONCLUSIONS

The results of our ESR measurements have demonstrated the importance of the exchange interactions in $NdGa_2$. In the absence of exchange one expects to observe resonances of the conduction electrons as well as those of the f electrons for the given CEF energy-level scheme. The presence of the sf exchange increases the Zeeman splitting of the energy levels so that the f-electron resonances are shifted outside the range of the X-band experiment. This was indeed observed in $NdGa_2$ where only the conduction-electron resonances have been detected. At low temperatures the spectrum width and the ESR susceptibility are dominated by the sf exchange interaction. The $4f$-electron Curie-Weiss susceptibility χ_{4f} gives the dominant contribution to the intensity of the conduction-electron line via the sf coupling and enhances the conduction-electron susceptibility so that the T dependences of χ_{ESR} and the sf exchange coupling parameter $C(T)$ below 80 K follow approximately that of χ_{4f}. The f-electron magnetism is thus observed indirectly via the enhancement effect on the conduction electrons.

Magnetization measurements with a SQUID magnetometer have demonstrated that the origin of the reported ferromagnetic component at low T is not from a true FM state. Instead, the magnetization is field induced and decays to zero after switching off the external magnetic field. A nonresonant microwave absorption, reported previously for canted antiferromagnets, has also been observed in $NdGa_2$ below T_N.

[1] D. Gignoux, D. Schmitt, A. Takeuchi, and F. Y. Zhang, J. Magn. Magn. Mater. **97**, 15 (1991).

[2] A. R. Ball, D. Gignoux, and D. Schmitt, J. Magn. Magn. Mater. **119**, 96 (1993).

[3] A. R. Ball, D. Gignoux, A. P. Murani, and D. Schmitt, Physica B **190**, 214 (1993).

[4] A. R. Ball, D. Gignoux, J. Rodriguez Fernandez, and D. Schmitt, J. Magn. Magn. Mater. **137**, 281 (1994).

[5] T.-H. Tsai and D. J. Sellmyer, Phys. Rev. B **20**, 4577 (1979).

[6] J. A. Blanco, D. Gignoux, J. C. Gomez Sal, J. Rodriguez Fernandez, and D. Schmitt, J. Magn. Magn. Mater. **104-107**, 1285 (1992).

[7] Y. Aoki, H. Sato, and H. Sugawara, Physica B **230-232**, 770 (1997).

[8] A. R. Ball, D. Gignoux, and D. Schmitt, Physica B **180-181**, 58 (1992).

[9] J. A. Blanco, D. Schmitt, and J. C. Gómez Sal, J. Magn. Magn. Mater. **116**, 128 (1992).

[10] P. Vonlanthen, J. L. Gavilano, B. Ambrosini, H. R. Ott, Y. Aoki, H. Sugawara, and H. Sato, Eur. Phys. J. B **9**, 15 (1999).

[11] A. Furrer and O. E. Martin, J. Phys. C **19**, 3863 (1986).

[12] K. W. H. Stevens, Proc. Phys. Soc. London, Sect. A **65**, 209 (1952).

[13] J. Winter, *Magnetic Resonance in Metals* (Clarendon, Oxford, 1971), p. 158.

[14] F. B. Hagedorn, E. M. Gyorgy, R. C. LeCraw, J. C. Hensel, and J. P. Remeika, Phys. Rev. Lett. **21**, 364 (1968).

[15] Andrew Ball, Ph.D. thesis TS 93/GRE1/0075, University Joseph Fourier, Grenoble, France, 1993, p. V-220.